Received: 28 February 2024 | Revised: 1 June 2024 | Accepted: 25 June 2024

DOI: 10.1111/jnc.16173

Journal of Neurochemistry JNC The Official Journal of the International Society for Neurochemistry WILEY

ORIGINAL ARTICLE

Organelle phenotyping and multi-dimensional microscopy identify C1q as a novel regulator of microglial function

Pooja S. Sakthivel[1,2] | Lorenzo Scipioni[3] | Josh Karam[1] | Zahara Keulen[1,4] | Mathew Blurton-Jones[1,4,5] | Enrico Gratton[3] | Aileen J. Anderson[1,2,5,6]

[1]Sue and Bill Gross Stem Cell Research Center, University of California, Irvine, California, USA

[2]Department of Anatomy and Neurobiology, University of California, Irvine, California, USA

[3]Laboratory for Fluorescence Dynamics, Biomedical Engineering, University of California, Irvine, California, USA

[4]Department of Neurobiology and Behavior, University of California, Irvine, California, USA

[5]Institute for Memory Impairments and Neurological Disorders University of California, Irvine, California, USA

[6]Department of Physical Medicine and Rehabilitation, University of California, Irvine, California, USA

Correspondence
Aileen J. Anderson, Sue and Bill Gross Stem Cell Research Center, University of California, Irvine, CA, USA.
Email: aja@uci.edu

Funding information
National Institutes of Health, Grant/Award Number: T32NS082174 and R01NS123927-01Q

Abstract

Microglia, the immune cells of the central nervous system, are dynamic and heterogenous cells. While single cell RNA sequencing has become the conventional methodology for evaluating microglial state, transcriptomics do not provide insight into functional changes, identifying a critical gap in the field. Here, we propose a novel organelle phenotyping approach in which we treat live human induced pluripotent stem cell-derived microglia (iMGL) with organelle dyes staining mitochondria, lipids, lysosomes and acquire data by live-cell spectral microscopy. Dimensionality reduction techniques and unbiased cluster identification allow for recognition of microglial subpopulations with single-cell resolution based on organelle function. We validated this methodology using lipopolysaccharide and IL-10 treatment to polarize iMGL to an "inflammatory" and "anti-inflammatory" state, respectively, and then applied it to identify a novel regulator of iMGL function, complement protein C1q. While C1q is traditionally known as the initiator of the complement cascade, here we use organelle phenotyping to identify a role for C1q in regulating iMGL polarization via fatty acid storage and mitochondria membrane potential. Follow up evaluation of microglia using traditional read outs of activation state confirm that C1q drives an increase in microglia pro-inflammatory gene production and migration, while suppressing microglial proliferation. These data together validate the use of a novel organelle phenotyping approach and enable better mechanistic investigation of molecular regulators of microglial state.

KEYWORDS
C1q, complement, inflammation, microglia, organelles

1 | INTRODUCTION

As the immune cells of the central nervous system (CNS), microglia are constantly surveying the microenvironment via dynamic processes and protrusions to facilitate a rapid response to damage (Nimmerjahn et al., 2005). In response to neuropathological stimuli (such as CNS disease or injury), microglia respond within minutes by transitioning states via functional reprogramming (Hakim et al., 2021). While it is well-understood that microglial state is not binary as once believed (Ransohoff, 2016), many microglial

Abbreviations: ADRC, Alzheimer's Disease Research Center; CNS, central nervous system; iMGL, induced pluripotent stem cell-derived microglia; LPS, lipopolysaccharide; scRNAseq, single cell RNA sequencing.

Laboratory of Origin: Anderson lab (University of California, Irvine); 845 Health Sciences Road, Irvine, CA 92617.

subpopulations that appear after disease/injury are associated with an inflammatory gene signature. These microglia release proinflammatory cytokines that are critical for the initial response to disease; however, prolonged cytokine release at the chronic stage of disease can inhibit neural repair and contribute to worsened pathology (Block et al., 2007; Polazzi & Contestabile, 2002; Zhang, 2011). Despite the notion that microglial inflammation heavily influences disease recovery, it remains unclear what molecular mechanisms regulate microglial inflammatory subpopulations in the healthy and diseased CNS.

One potential molecular regulator of interest is C1q, the initiator molecule of the complement cascade. While C1q is traditionally known for its role in the immune system, it has recently become recognized for novel functions as a single molecule within the CNS. For example, C1q can regulate neurodevelopment (Schafer et al., 2012; Stevens et al., 2007) and neurite outgrowth (Peterson et al., 2015). Here, we investigate a novel role for C1q in regulating microglial state and function. C1q protein increases by 300-fold in the aged versus control brain (Stephan et al., 2013) and further accumulates within the context of neurodegeneration (Yasojima et al., 1999), highlighting the potential for C1q to influence CNS cells as a paracrine signal. Indeed, one previous study found that C1q drives release of inflammatory cytokines (TNFα and IL-6) in rat microglia primary cultures (Färber et al., 2009). In parallel with its traditional role within the complement cascade, we hypothesize that C1q is a molecular cue for regulating human microglial function and inflammation within the diseased CNS.

Critically, technological limitations have historically made it difficult to assess microglial responses to treatment or disease at the resolution needed to discern complex heterogeneity. Recent advances in single-cell RNA sequencing (scRNAseq) allow for identification of numerous context-dependent microglial subpopulations, for example, inflammatory and anti-inflammatory microglia (Michelucci et al., 2009), disease-associated microglia (Keren-Shaul et al., 2017), interferon-responsive microglia (Sala Frigerio et al., 2019), and white matter-associated microglia (Safaiyan et al., 2021). While scRNAseq is a powerful tool for identifying microglial heterogeneity and highlighting pertinent signaling pathways, these naming conventions label subpopulations based on transcriptomic signature without addressing the fundamental question of microglia function. Additionally, there are a number of caveats with scRNAseq that limit its applications, including: (1) gene expression does not predict the function of identified subpopulations; (2) transcriptomic changes often do not correlate with protein (Koussounadis et al., 2015); and (3) technical limitations do not allow for detection of lowly transcribed genes. Critically, evaluation of microglial functional heterogenetiy at the single cell level remains a major gap in the field (Paolicelli et al., 2022).

Here, we test a novel functional-based organelle phenotyping approach via multidimensional microscopy (Scipioni et al., 2024) to evaluate microglia organelles at a single-cell level. In contrast with traditional transcriptomic or proteomic techniques, organelle phenotyping quantifies real-time functional changes in energetic and anabolic metabolism. Microglia are labeled with environment-sensitive dyes for mitochondria, lysosomes, and lipids and data are acquired in live cells by spectral microscopy. This combination of organelle dyes and live microscopy allows for functional and morphological changes to be probed in individual, live cells following treatment. We validated this approach using human induced pluripotent stem cell-derived microglia (iMGL) and quantification of cellular changes in response to the classical stimulants lipopolysaccharide (LPS) and IL-10. Furthermore, we applied this functional phenotyping approach to test the hypothesis that purified human C1q also influences microglial organelle function. Overall, we identified that C1q influences microglial function via multiple quantitative endpoints: organelles, gene expression, proliferation, and migration. These data highlight the capacity of organelle phenotyping to identify new molecules that regulate microglial state, and suggest a novel function for C1q as a single ligand separate from its traditional role in the complement cascade.

2 | MATERIALS AND METHODS

2.1 | Acquisition and maintenance of iPSC

UCI Alzheimer's Disease Research Center (ADRC)76 cell line was obtained from human fibroblasts to generate iPSC. The cell line was derived from subject 76 (male) with informed consent; reprogramming and differentiation was approved by the University of California, Irvine Institutional Review Board. iPSC use and differentiation towards microglia was approved by the University of California, Irvine Human Stem Cell Research Oversight Committee (hSCRO protocol # 3682).

iPSC were plated onto 6-well plates (Corning cat#08-772-1B) coated with growth factor-reduced Matrigel (1 mg/mL; BD Biosciences, cat#356231). iPSC cell maintenance involves daily media changes in mTeSR Plus (Stem Cell Technologies, cat#100-0276) and a humidified incubator (5% CO_2, 37°C). Medium was supplemented with 0.5 μM Thiazovivin (StemCell Technologies, cat#72252) for the first 24 h post-passage to promote colony survival. iPSC were tested for mycoplasma every 3 months and were confirmed to be negative.

2.2 | Differentiation of microglia from iPSC

iPSC were differentiated into microglia using a previously published protocol (McQuade et al., 2018). Briefly, iPSC were passaged in a 6-well plate with mTeSR Plus at a density of 40–80 small colonies (<100 cells) per well. iPSC-derived hematopoietic progenitor cell differentiations were completed with STEMdiff Hematopoietic Kit (Stem Cell Technologies, cat#5310) where cells are fed with Media A (day 0–2) and Media B (day 3–10). Non-adherent CD43+ iHPC are collected on days 11/12 and plated in iMGL medium (Table 1), freshly supplemented with 100 ng/mL IL-34 (Peprotech, cat#200-34), 50 ng/mL TGFb1 (Peprotech, cat#100-21), and 25 ng/mL M-CSF

TABLE 1 Components of iMGL media.

Product	Manufacturer
DMEM/F12	Gibco, #1103901
Insulin-Transferin-Selenite	Gibco, #41400045
2× B27	Gibco, #17504044
0.5× N2	Gibco, #17502048
1× Glutamax	Gibco, #35050061
1× NEAA	Gibco, #11140050
400 mM monothioglycerol	Sigma, #M6145
5 μg/mL human insulin	Sigma, #I2643

(Peprotech, cat#300-25) for 28 days. The last 3 days in culture involve feeding in iMGL maturation media, which is iMGL medium freshly supplemented with 100 ng/mL CD200 (Novoprotein, cat#BP004) and 100 ng/mL CX3CL1 (Peprotech, cat#300-18). Mature iMGL were treated with 100 ng/mL LPS (ThermoFisher Scientific, cat#00-4976-03), 10 ng/mL IL-10 (R&D Systems, cat#21-7IL0-10), or C1q[1–200 nM] (My Biosource, cat#MBS147305) as described.

2.3 | Microglia organelle phenotyping

Following 24-h treatment, iMGL were processed and data were analyzed as previously described (Scipioni et al., 2024). Briefly, cells were labeled with the following environment-sensitive dyes to observe changes in organelles: TMRM (mitochondrial membrane potential), Lysotracker Green (lysosomal pH), Lipi-Blue (lipid droplet polarity), and SiR-Hoechst (DNA). Live-cell data were acquired using a Zeiss LSM880 confocal microscope with hyperspectral (Quasar) detection. Cells were images with a 63×/1.4 NA Oil objective, single-cell segmentation was achieved via Cellpose using the "cyto2" pretrained convolutional neural network. All data analyses were performed in Python.

2.4 | qPCR

Following treatment, cells were lysed using RLT buffer mastermix (10 μL beta-mercaptoethanol: 1 mL RLT) and cells were lysed with RNAeasy micro kit (Qiagen, 74004). RNA quality and quantity was validated using a nanodrop (ThermoFisher Scientific). Any remaining genomic DNA from the collected samples was degraded using RNA clean up kit (Invitrogen, cat#:AM1906). RNA samples were then converted to cDNA using high-Capacity RNA-to-cDNA kit (Applied Biosystems, cat#:4387400). qPCR reaction was performed in a 10 μL volume using the qPCR primers listed in Table 2 (ThermoFisher Scientific, cat#: 4448892). Reaction included 20× TaqMan Gene Expression Primer, 2× TaqMan Gene Expression Fast Mastermix (Applied Biosystems, cat#:4444557), cDNA template, and RNAse free water. Plate was sealed, centrifuged briefly, and loaded into Quantstudio7. Data were analyzed using the comparative delta–delta Ct method.

TABLE 2 qPCR primers used to evaluate microglial gene signature.

Gene	Assay ID
18 s	Hs03003631_g1
CCL2	Hs01574247_m1
IL1b	Hs01555410_m1
IL6	Hs00174131_m1
IL-10	Hs00961622_m1
BDNF	Hs02718934_s1
IGF1	Hs01547656_m1
P2RY12	Hs01881698_s1
SELPLG	Hs05033974_s1
CX3CR1	Hs01922583_s1

2.5 | Transwell migration assay

iMGL were collected and resuspended to a concentration of 300000 cells/mL. 30000 cells (100 μL) of the single-cell resuspension was added to each migration assay chamber, before placing chambers into feeder trays (Millipore) containing 150 μL of media for each condition; the chambers were then incubated at 37°C for 3 hr. Subsequently, the chambers were transferred onto new 96-well trays containing 150 mL of prewarmed cell detachment buffer and incubated for 30 min at 37°C. At the end of this incubation, 50 mL 1:75 dilution of CyQuant GR Dye:Lysis buffer was added to the cell detachment buffer and incubated for 15 min at room temperature. Finally, 150 mL CyQuant GR Dye:Lysis/detachment solution was transferred to a new 96-well plate, and migration was quantified using a 480/520 nm filter set on a fluorescent plate reader. All experiments were conducted in biological triplicate with technical triplicates.

2.6 | Flow cytometry (Click-it EdU and AnnexinV)

All samples were acquired on the BD Fortessa and data were analyzed using FloJo. All experiments were conducted in biological triplicate and technical triplicate. EdU: Cell proliferation was assessed using flow cytometric detection of EdU incorporation. iMGL were incubated with EdU (Cayman, cat#: 20518) 1:000 for 24 h in combination with treatment in the incubator. iMGL were collected and fixed with 4% PFA for 15 min prior to detection with the Click-iT™ Plus Alexa Fluor™ 488 Picolyl Azide Toolkit (Invitrogen, cat#: C10641). Briefly, cells were washed in PBS-1%FBS and permeabilized with 0.1% saponin in PBS-1%FBS for 15 min before incubation with staining solution [1x click-it reaction buffer, CuSO4, AF488 picolyl azide, and 1x additive] for 45 min at room temperature. Cells were once again

washed with PBS-1% FBS before acquisition. Annexin: Apoptosis was assessed using PE Annexin V Apoptosis Detection Kit with 7-AAD (Biolegend, cat#: 640934). iMGL were collected and washed twice with Biolegend's cell staining buffer. Cells were resuspended in 100 μL Annexin V binding buffer and treated with PE Annexin V 1:20 and 7-AAD viability staining solution 1:20. Antibodies were incubated for 15 min room temperature and 400 μL of Annexin C binding buffer was added to each tube before acquisition.

2.7 | Apolive Glo cell viability/apoptosis assay

iMGL viability and apoptosis was quantified with ApoLive-Glo™ Multiplex Assay (Promega, cat#: G6410) per manufacturer's instructions. Briefly, iMGL were treated with GF-AFC, a cell-permeant substrate that becomes fluorescent when it enters the cell to quantify viable cells. Then, cells are lysed and treated with a luminogenic caspase-3/7 substrate to quantify amount of caspase present. Data are shown as caspase luminescence/live cell fluorescence as a normalization measure. All experiments were conducted in $n = 3$ biological replicates and $n = 5$ technical replicates.

2.8 | Statistical analysis

Statistical analyses were performed using Prism GraphPad Prism version 10. The number of biological replicates (n), statistical tests conducted, and statistical significance are indicated in all figure legends. All data are expressed as mean ± standard error of the mean. Data collection and analysis were performed by investigators blinded to experimental groups. One-way ANOVA, followed by Tukey's multiple comparisons when appropriate, was used for all statistical analyses following confirmation of normality by Kolmogorov–Smirnov tests (alpha = 0.05). Figure 5a was additionally analyzed by one sample t-test to compare between untreated control and each C1q treatment. No outlier tests were performed.

3 | RESULTS

3.1 | Organelle phenotyping and multidimensional microscopy identify functional microglial subpopulations in an unbiased manner

Microglia undergo rapid transcriptomic changes in response to various molecular cues. However, changes in microglial organelles and their downstream impacts on cellular function (particularly in a single-cell, high throughput manner) are much less understood. Microglial state is associated with changes in metabolism, such as a mitochondrial shift towards glycolysis (Voloboueva et al., 2013), and an increase in acidic lysosomes (Majumdar et al., 2007) and lipids (Button et al., 2014). Because organelle changes are integrally linked to cell metabolism, these readouts can provide direct insight into cell function. We therefore hypothesize that organelle phenotyping and multidimensional microscopy can identify microglial subpopulations by probing changes in microglial organelles as an alternative output to study activation.

As a validation for this methodology, iMGL either remained untreated as a negative control, or were treated with LPS or IL-10 for 24 h. Although we acknowledge microglia are non-binary cells, the extreme ends of microglial heterogeneity can be described via the "inflammatory" and "anti-inflammatory" nomenclature. Because LPS and IL-10 have traditionally been used to polarize microglia to these states, we used these treatments as positive controls to investigate whether this methodology could identify microglial subpopulations in an unbiased manner. Because a previous study suggested a role for C1q in regulating cytokine release in rodent microglia (Färber et al., 2009), iMGL were also treated with purified C1q to test the hypothesis that C1q similarly regulates human microglial state and function. We predicted that C1q would polarize microglia towards an inflammatory phenotype, and thus expected to observe a similar but distinct pattern when compared to LPS-treated cells. In addition to these treatments, iMGL were labeled with the following environment-sensitive dyes for 1 h to observe changes in organelles while triggering minimal dye toxicity: TMRM (mitochondrial membrane potential), Lysotracker Green (lysosomal pH), Lipi-Blue (lipid droplet polarity), and SiR-Hoechst (DNA; Figure 1a–d). Multicolor images were acquired using live-cell hyperspectral microscopy, allowing for quantification of organelle characteristics with single-cell resolution in a single image.

Once the hyperspectral was acquired, images of the single organelles were unmixed by phasor spectral unmixing and intensity histogram, and auto- and cross-correlation curves were extracted using image (cross-)correlation spectroscopy. Individual bins of the intensity histograms and correlation curves were area-normalized and used as organelle features, similarly to gene expression profiles in scRNA-seq. Feature extraction was followed by PacMAP dimensionality reduction and unbiased subpopulation identification by Gaussian Mixture Model clustering. The optimal number of clusters was identified by minimizing the Davies–Bouldin Index. Clusters represent groups of cells with distinct organelle characteristics and therefore distinct functions of the organelle network. The data revealed eight distinct microglial subpopulations (Figure 1e). We first visualized the proportion of each cluster based in each treatment group; that is, 30% of all C1q-treated cells were associated with cluster 0 (Figure 1f). These data show how certain clusters are predominantly associated with treatment groups. PacMAP can alternatively be visualized by treatment (Figure 1g), highlighting how treatments differentially influence cells, and identifying that untreated cells cluster separately from treated cells. Moreover, we can similarly visualize the proportion of each treatment within each cluster; that is, 66% of cluster 0 is made up of C1q-treated cells (Figure 1h). These data revealed that clusters 3 and 7 were largely made up of IL-10 treated cells, whereas cluster 4 identified many untreated cells. Cluster 6 was equally comprised of all four treatment groups, suggesting that it may represent a baseline homeostatic or trophic subpopulation

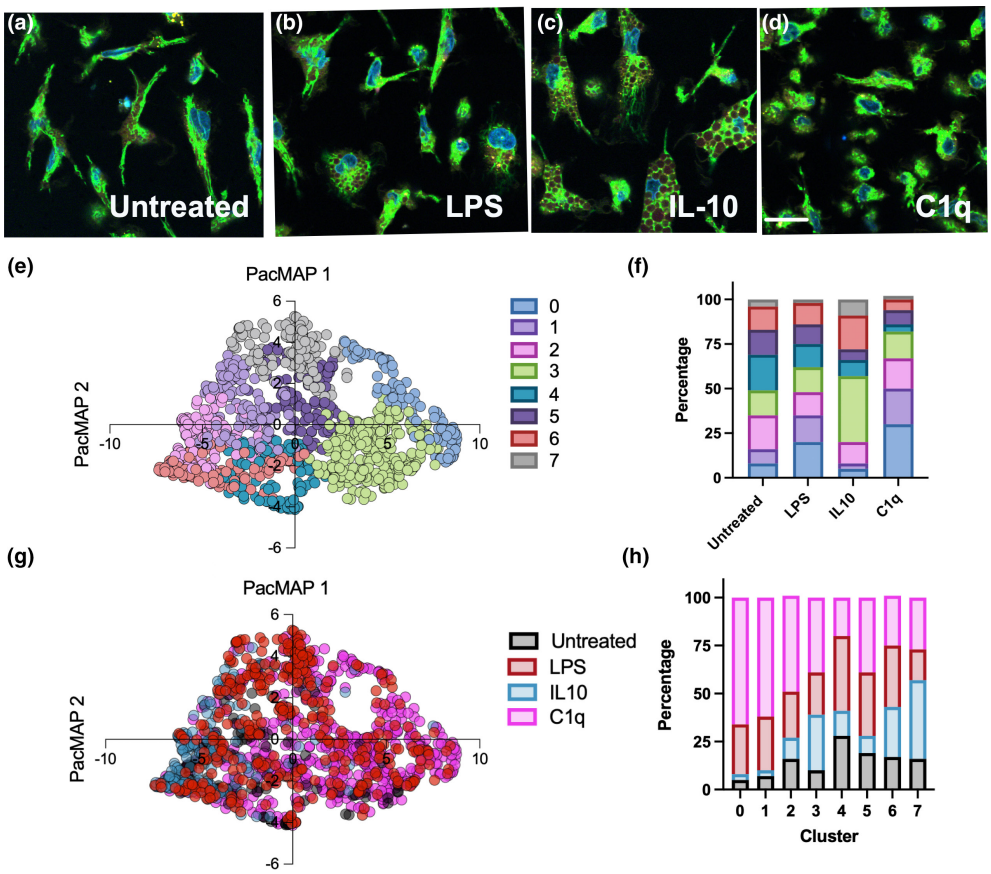

FIGURE 1 C1q triggers changes in iMGL organelles and morphology, similar to LPS. (a–d) iMGL remain untreated as a control (a) or are treated with lipopolysaccharide (LPS) (b), IL-10 (c), or C1q (d). Cells are labeled with lysotracker green (lysosomes, red), lipi-blue (lipids, yellow), TMRM (mitochondria, green), and SiR-hoechst (DNA, blue). Live cells are imaged 24 h following treatment. (e–h) Data acquisition is followed by PacMAP dimensionality reduction and cluster identification, revealing eight distinct cluster that are associated with treatments (e, g). Cluster composition by treatment (f) and treatment composition by cluster (h) show cluster analysis is able to recognize heterogeneity and functional changes driven by treatment in an unbiased manner. $n = 1296$ microglia, three biological replicates. Scale bar = 30 μm.

present regardless of treatment. Critically, four out of eight clusters (0, 1, 2, and 5) were associated predominantly with C1q and LPS-treated iMGL; the observation that these clusters shared identification between C1q and LPS-treated cells suggests that C1q drives changes in organelle function that are consistent with a classical proinflammatory phenotype. In sum, organelle phenotyping identified changes in microglia in response to treatment, and PacMAP followed by unbiased cluster identification was able to read out distinct cell subpopulations in an unbiased manner. These data support organelle phenotyping as a useful methodology for characterizing microglial state based on function.

3.2 | C1q drives complex changes in iMGL morphology and organelle function

Cell morphology is one the first prominent changes observed in microglia within the diseased CNS (Nimmerjahn et al., 2005). While homeostatic microglia are typically branched, activated microglia are known to adopt larger cell volume and decreased branching complexity. As expected, live-cell imaging highlights striking morphological changes following treatment with LPS, IL-10, or C1q. Figure 2 shows low-power images of microglia following treatment and categorization of each individual cell into a corresponding cluster. Untreated microglia (Figure 2a,b) displayed a classical long and branching morphology which is essential for surveillance of the microenvironment and quick response to signs of disease. Conversely, microglia in response to treatment displayed several distinct morphological changes consistent with an "activated" phenotype. A subpopulation of microglia treated with LPS (Figure 2c,d) showed classical ameboid morphology—round, small, and circular. Moreover, few microglia adopted a slimmer elongated morphology that retained branching following LPS treatment. Because rod-shaped morphology has previously been described as an intermediate transition state between a branched and amoeboid microglia (Au & Ma, 2017), LPS-treated microglia may be displaying this elongated morphology before transitioning towards the classical amoeboid state. In contrast, IL-10 drove a much larger, non-circular shaped microglia (Figure 2e,f). Notably, C1q-treated microglia more consistently showed a classical activated, ameboid morphology that

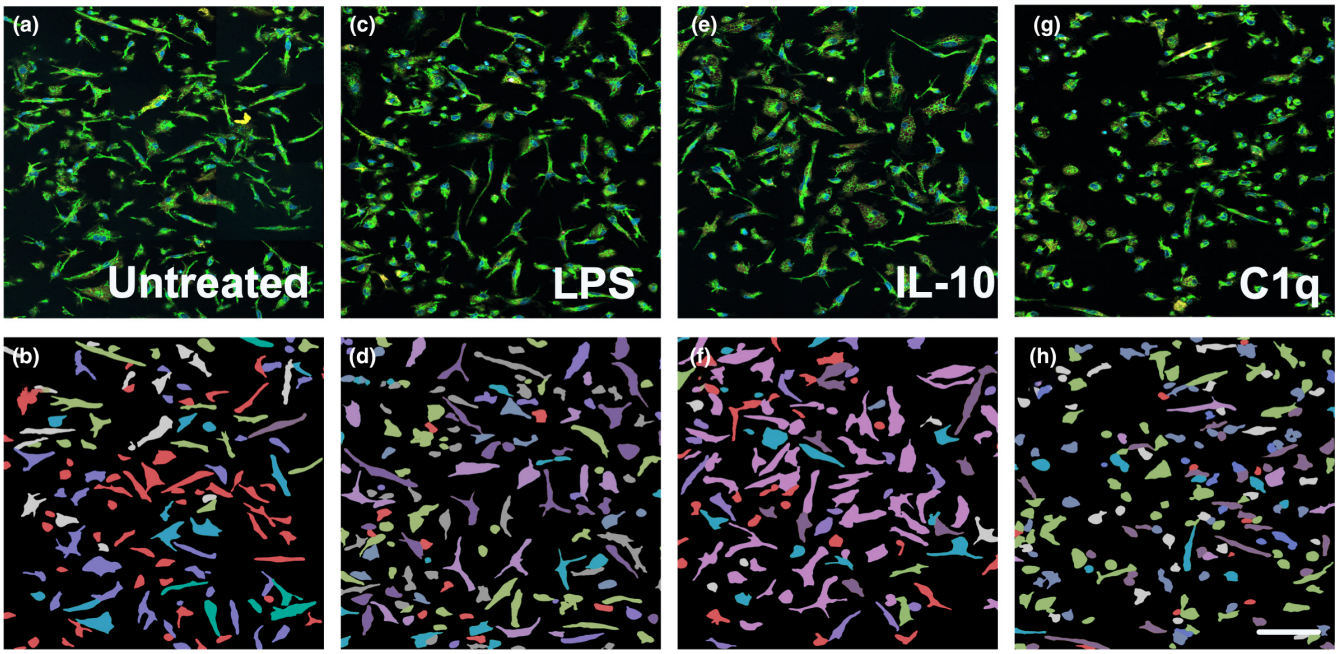

FIGURE 2 All stimulants trigger distinct changes in iMGL morphology. iMGL remain untreated as a control (a, b) or are treated with lipopolysaccharide (LPS) (c, d), IL-10 (e, f), or C1q (g, h). lysotracker green (lysosomes, red), lipi-blue (lipids, yellow), TMRM (mitochondria, green), and SiR-hoechst (DNA, blue). Live cells are imaged 24 h following treatment. (a, c, e, g) show low power image of microglia following treatment and (b, d, f, h) show cells highlighted by identified cluster. $n = 1296$ microglia. Scale bar = 100 μm.

is small and circular (Figure 2g,h). Organelle phenotyping therefore provides high throughput morphological data at the single-cell level, ultimately allowing for morphological changes to be correlated with functional changes within identified subpopulations.

iMGL subpopulations identified by cluster analysis were further analyzed to identify which characteristics drive cluster separation, providing unbiased insight into which characteristics are most different across cell treatments and clusters. As expected, morphological differences based on cell area and solidity (a readout of how circular a cell is) were two characteristics that drove cluster separation. IL-10 drove an increase, and C1q drove a decrease in cell area, whereas LPS did not influence overall cell area (Figure 3a). Moreover, IL-10 drove a decrease in solidity (increase in branching), and C1q drove an increase in solidity (decrease in branching), whereas LPS did not influence cell solidity in comparison to untreated cells (Figure 3b). Quantification of additional morphological readouts may have revealed physical alterations associated with LPS treatment; consistent with this interpretation, an unpaired *t*-test between untreated solidity and LPS solidity revealed a statistically significant increase ($p = 0.0373$), suggesting LPS does trigger a slight decrease in microglial branching. Overall, these data suggest that LPS, IL-10, and C1q may function through different mechanisms and thereby have discrete impacts on cell morphology and function.

Accumulation of fat storage and lipid droplets are often associated with inflammation and activation in immune cells (D'Avila et al., 2008). Indeed, LPS drove an increase in fatty acid storage (Figure 3c), as has been previously noted in the literature for murine microglia (Khatchadourian et al., 2012). Consistent with the predication that IL-10 would drive the converse effect, IL-10 treated microglia displayed a slight decrease in fatty acid storage (Figure 3c). Furthermore, C1q displayed an increase in fatty acid storage that was comparable to LPS. These data together show that LPS and C1q influence microglial fatty acid storage similarly, while IL-10 drives the opposite phenotype.

As the primary phagocytes within the CNS, microglial lysosomes are indicative of phagocytosis and digestion. Indeed, an increased number of microglial lysosomes has been consistently noted in the context of neurodegeneration and neuroinflammation (Quick et al., 2023). While both LPS- and IL-10-treated microglia display an increase in lysosomes (Figure 1b,c), only IL-10-treated microglia display a significant increase in lysosome acidity (Figure 3d). This is consistent with previous findings showing IL-10 treatments increase phagocytic capacity of microglia (Yi et al., 2020). Interestingly, autophagy is known to regulate lipid metabolism (Singh et al., 2009) and IL-10-treated microglia accordingly show a stark decrease in fatty acid storage (Figure 3c). These data highlight the complexity of organelle function and its influence on microglial state, moreover highlighting the value of this tool in studying how microglial organelles change in the context of disease.

We next investigated intensity of SiR-Hoechst (DNA stain) as a characteristic that separates out the identified subpopulations (Figure 3e). We observed a significant decrease in SiR-Hoechst intensity following IL-10 treatment, suggesting chromatin unfolding. This is validation of IL-10 and its influence on epigenetic modifications that has previously been noted in the literature (Rajbhandari

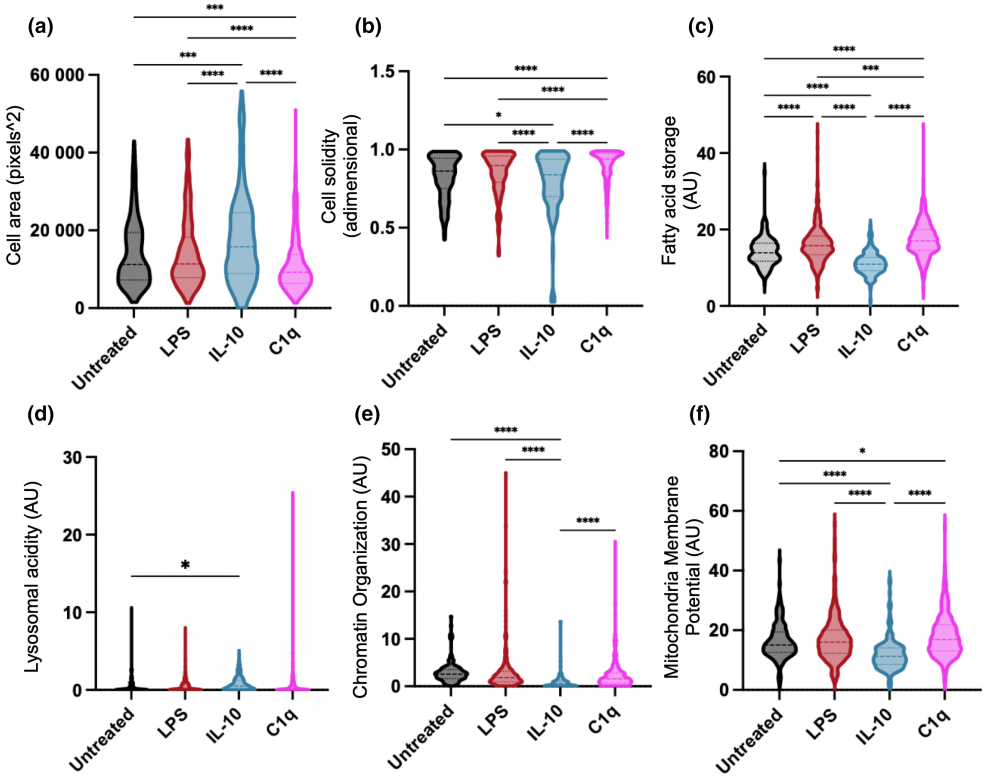

FIGURE 3 Functional changes in microglial organelles drive cluster separation. Subpopulation identification in an unbiased manner is largely due to changes in microglial morphology (a, cell area; b, cell solidity) and lipids (c), lysosome acidity (d), chromatin organization (e), and mitochondria membrane potential (f) in arbitrary units (AU). Statistical analysis by one-way ANOVA: [Cell area] $F(3, 1292) = 21.25$, $p \leq 0.0001$; [Cell Solidity] $F(3,1292) = 22.89$, $p \leq 0.0001$; [Fatty Acid Storage] $F(3,1298) = 10.13$, $p \leq 0.0001$; [Lysosomal Acidity] $F(3,1291) = 2.192$, $p = 0.0207$; [Chromatin Organization] $F(3,1292) = 5.965$, $p = 0.0001$; [Mitochondria Membrane Potential] $F(3,1292) = 6.865$, $p \leq 0.0001$. Post-hoc Tukey's *t*-test as indicated. $^{*}p \leq 0.05$, $^{***}p \leq 0.001$, $^{****}p \leq 0.0001$. $n = 1296$ microglia, three technical replicates.

et al., 2018). Chromatin changes following LPS treatments have also been noted in other cell types (Shen et al., 2016). However, our data do not show a significant increase in SiR-Hoechst intensity in either LPS or C1q treatment. These data could suggest DNA compaction is influenced in anti-inflammatory microglia and that DNA/chromatin is a meaningful output to observe when considering epigenetics influence on microglial state.

Last, we evaluated changes in mitochondrial membrane potential across treatments (Figure 3f). LPS did not change TMRM intensity, while IL-10 drove a significant decrease, and C1q drove a significant increase. Interestingly, this is one organelle phenotype where LPS and C1q displayed separate responses, suggesting C1q likely promotes microglial oxidative phosphorylation and ATP production in a manner that is distinct from LPS. These differing observations across all treatments highlight the variable changes in energy dynamics and the need for a functional output like mitochondria membrane potential. Moreover, these data show that C1q influences microglial inflammation likely through a different mechanism from LPS and that organelle phenotyping has the capacity to quantify both the similarities and differences between these two treatments. In summary, we demonstrate that organelle phenotyping can be used to interrogate multiple organelle outputs associated with microglial state in an unbiased manner, and we apply it to show C1q induces microglial organelles to exhibit characteristics consistent with a proinflammatory phenotype.

3.3 | C1q drives an inflammatory gene signature in iMGL, as predicted by the organelle changes observed with multidimensional microscopy

Because LPS- and C1q-treated iMGL show similar trends in organelle phenotyping, we predicted that LPS and C1q treated iMGL would also show similar trends in RNA production, a readout that is more historically used to evaluate microglial state. We thus used qPCR as a more traditional evaluation of gene expression to assess microglial state and quantify three representative inflammatory, anti-inflammatory, and homeostatic genes. To additionally investigate a dose–response, iMGL were treated with three physiologically relevant concentrations of C1q produced by neutrophils [0.1 nM], macrophages [1 nM], and its concentration in the blood/serum [200 nM] (Hooshmand et al., 2017). After a 24-h C1q treatment, iMGL were lysed and mRNA was isolated for qPCR to investigate changes in transcription. Consistent with LPS, C1q also triggered an upregulation of inflammatory genes (CCL2, IL1-β, and IL-6) in a dose-dependent manner (Figure 4a). These data confirm that C1q

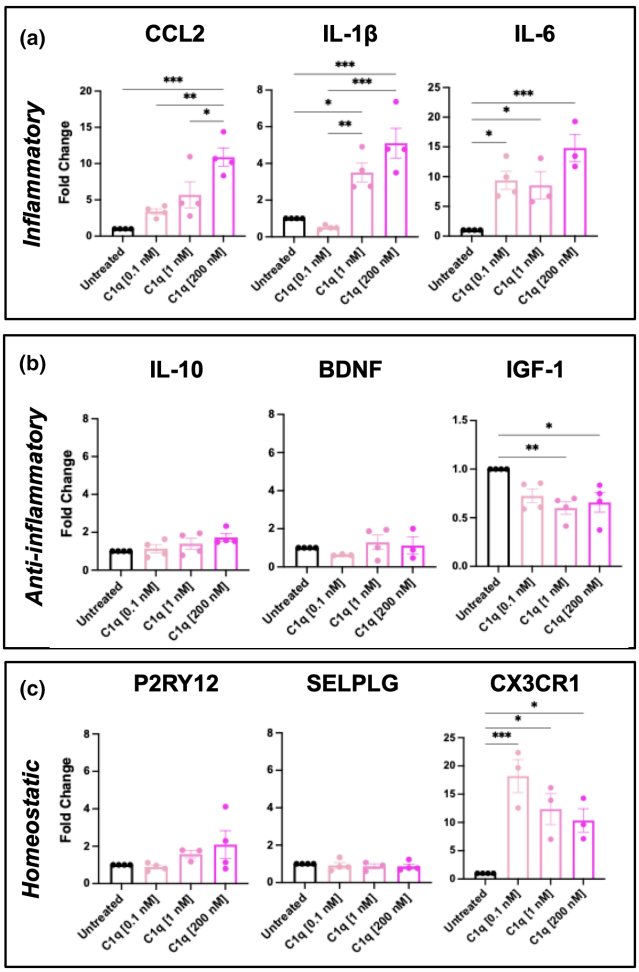

FIGURE 4 Paracrine C1q drives an inflammation-associated transcriptional signature. iMGL are treated with C1q at three physiologically relevant concentrations: 0.1, 1, and 200 nM. Cells are lysed following 24-h treatment and mRNA is collected to investigate (a) inflammatory, (b) anti-inflammatory, and (c) homeostatic gene expression. Data show mean ± SEM normalized to untreated controls. Statistical analysis by one-way ANOVA: [CCL2] $F(3, 12) = 1.144$, $p \leq 0.0003$; [IL-1b] $F(3, 12) = 1.975$, $p \leq 0.0001$; [IL-6] $F(3, 10) = 1.101$, $p \leq 0.001$; [IL-10] $F(3, 12) = 4.053$, $p = 0.1203$; [BDNF] $F(3, 10) = 3.947$, $p = 0.04$; [IGF-1] $F(3, 12) = 2.117$, $p = 0.0074$; [P2RY12] $F(3, 11) = 4.403$, $p = 0.1918$; [SELPLG] $F(3, 11) = 0.7597$, $p = 0.8368$; [CX3CR1] $F(3, 9) = 1.188$, $p = 0.0012$. Tukey's *t*-test as indicated. $^{*}p \leq 0.05$, $^{**}p \leq 0.01$, $^{***}p \leq 0.001$. $n = 3$ technical replicates per 3–4 biological replicates.

increases the expression of inflammatory genes, in support of our prediction. Thus, the microglial phenotypes identified with multidimensional microscopy (Figure 1) are correlated with changes in gene expression that are associated with an inflammatory state.

We additionally probed whether C1q changes the expression of representative anti-inflammatory or homeostatic genes. C1q had no effect on the anti-inflammatory genes IL-10 and BDNF, but slightly decreased the anti-inflammatory marker IGF-1 (Figure 4b). These data suggest that C1q can also decrease anti-inflammatory genes to promote an inflammatory phenotype. Lastly, C1q did not influence the homeostatic genes P2RY12 and SELPLG. However, C1q did drive an increase in CX3CR1 (Figure 4c). While CX3CR1 has historically been thought of as a homeostatic marker, CX3CR1 has recently been implicated in inflammatory processes as well (Freria et al., 2017; Ho et al., 2020). Interestingly, CX3CR1 has a known role in regulating phagocytosis (Zabel et al., 2016), thus, this may be a mechanism underlying C1q-driven phagocytosis, consistent with the traditional function of C1q (Fraser et al., 2010). Overall, these data demonstrate that paracrine C1q influences human iMGL to adopt an inflammatory gene signature and are consistent with previous reports of C1q influencing rodent microglia to release inflammatory cytokines (Färber et al., 2009), suggesting the role of C1q as an inflammatory cue is conserved across species.

3.4 | C1q triggers iMGL chemotaxis and phagocytosis, while attenuating iMGL proliferation

Microglia are well-known to rapidly respond to changes in homeostasis by migrating towards regions of disease, proliferating, and/or inducing apoptosis. We therefore lastly evaluated iMGL responses to C1q via quantitative assays that characterize microglial functions distinct from their transcriptomic signature, providing us with a better understanding of how C1q influences microglial behavior.

Because microglia are highly dynamic and motile cells within the CNS, we tested the hypothesis that C1q can serve as a chemotactic cue for iMGL. C1q is a known chemoattractant for numerous other cell types, including monocytes and macrophages (Agostinis et al., 2010; Kuna et al., 1996; Vogel et al., 2014). However, whether microglia migrate towards C1q remains unknown. iMGL were treated with all doses of C1q using a transwell migration assay. While all doses triggered chemotaxis, C1q[1 nM] interestingly induced increased migration when compared to C1q[0.1 nM] and C1q[200 nM] (Figure 5a). These data show for the first time that C1q drives microglial chemotaxis in a dose-dependent manner.

We also assessed cell proliferation via EdU incorporation and cell death via AnnexinV and 7-AAD expression following 24 h of C1q treatment. Quantification of iMGL that incorporated EdU into the DNA during the 24-h incubation period demonstrated that approximately 25% of iMGL proliferate/turnover at baseline; however, this was significantly reduced in the presence of C1q[200 nM] (Figure 5b). Moreover, quantification of AnnexinV+/7-AAD- iMGL and AnnexinV−/7-AAD+ iMGL (Figure 5c) revealed no change in apoptosis (Figure 5d) or necrosis (Figure 5e), respectively. These findings were independently replicated using the ApoliveGlo viability assay, which provides a luminescent readout of Caspase 3/7 activity as an alternative method to quantify apoptosis and cell viability (Figure 5d). Overall, we identify that C1q induced iMGL migration at all doses and attenuated iMGL proliferation at C1q[200 nM] only, but had no influence on iMGL apoptosis, necrosis, or cell viability. These data together show that C1q influences complex changes in microglial cell function by controlling migration and cell proliferation.

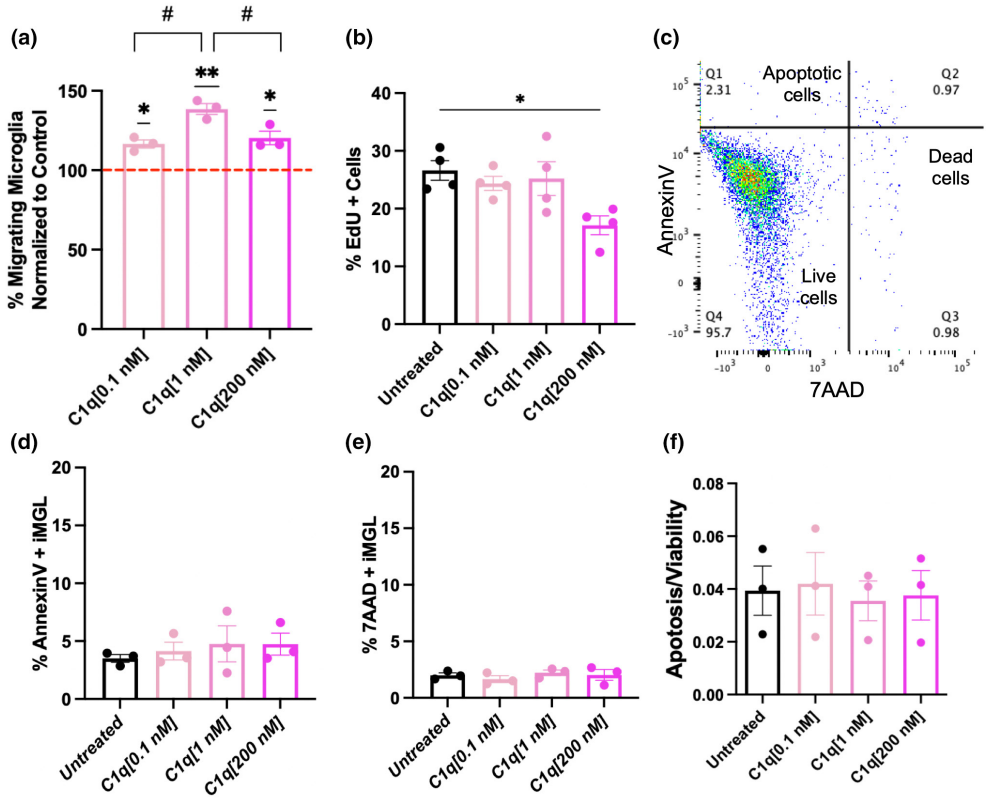

FIGURE 5 C1q influences microglial migration and proliferation, but not necrosis or apoptosis. (a) C1q[0.1 nM], C1q[1 nM], and C1q[200 nM] all induce iMGL chemotaxis in transwell migration assays. C1q[1 nM] induces an increased level of migration, in comparison to low and high C1q doses. Statistical analysis using one sample *t*-test (*$p \le 0.05$, **$p \le 0.01$) for comparison with untreated control and C1q treatments. Statistical analysis by using one-way ANOVA ($F(2, 6) = 0.06345$, $p = 0.0093$). Tukey's post-hoc *t*-test as indicated (#$p \le 0.05$) for comparison between conditions. $n = 3$ biological replicates. (b–f) iMGL are treated with C1q[0.1 nM], C1q [1 nM], or C1q[200 nM] for 24 h and processed to quantify proliferation and cell death. (b) C1q[200 nM] drives a significant decrease in the percentage of EdU+ cells in comparison to untreated iMGL. Statistical analysis by using one-way ANOVA ($F(3, 12) = 1.751$, $p = 0.023$). Tukey's post-hoc *t*-test as indicated for comparison between conditions. **$p \le 0.01$. $n = 4$ biological replicates. (c–f) C1q treatment does not influence microglia cell death via apoptosis or necrosis. Representative flow cytometry plot of AnnexinV and 7AAD staining shown in (c). (d) Quantification of AnnexinV+/7AAD- microglia reveals no change in apoptosis. Statistical analysis by one-way ANOVA (not significant, $F(3, 8) = 0.7259$, $p = 0.7867$). $n = 3$ biological replicates. (e) Quantification of Annexin-/7AAD+ microglia reveals no change in necrosis. Statistical analysis by one-way ANOVA (not significant, $F(3, 8) = 0.3042$, $p = 0.6683$). $n = 3$ biological replicates. (f) Quantification of apoptosis and viability by Apolive Glo assay also reveals no change in apoptosis following C1q treatment. Statistical analysis by one-way ANOVA not significant, $F(3, 8) = 0.1337$, $p = 0.9692$. $n = 3$ technical replicates per 3 biological replicates.

4 | DISCUSSION

Early studies in the mid-1970s first coined the term "microglial activation" when observing the striking difference in microglial morphology following brain damage (Tremblay et al., 2015). It is now understood that "microglial activation" is not black and white, and better tools are needed to evaluate these complex cells (Paolicelli et al., 2022). Here, we hypothesized that changes in organelles are a suitable methodology to investigate the wide spectrum of microglial polarization. Because it is well-understood that mouse models do not recapitulate the genomic changes observed in human inflammatory and neurodegenerative disorders (Burns et al., 2015; Seok et al., 2013), we used human iPSC and a protocol to differentiate them towards iMGL (McQuade et al., 2018). Previous work has demonstrated that the transcriptomic of these iMGL in vitro closely resemble the transcriptome of human microglia that have been rapidly isolated from brain biopsies without culturing (Hasselmann et al., 2019). Interestingly, recent single cell sequencing studies have shown that iMGL exhibit considerable heterogeneity in gene expression when cultured in vitro and these subpopulations can be efficiently mapped onto human brain-derived single cell sequencing datasets (Dolan et al., 2023).

We used iMGL to apply a novel multidimensional phenotyping technique based on hyperspectral microscopy to quantify changes in iMGL organelles and investigate microglial subpopulations in an unbiased, functionality-based manner. We demonstrate the capacity to quantify changes in microglial mitochondria, lipids, and lysosomes, as well as unbiased subpopulation clustering. We first tested the classical stimulants LPS and IL-10 to validate this functional phenotyping approach. We show that LPS increases lipid number, whereas IL-10 increases lysosomal pH and decreases mitochondria membrane potential. These data suggest inflammatory microglia are

likely to increase fat storage, whereas anti-inflammatory microglia increase lysosomal digestion and decrease energy production. We next applied this method to investigate the hypothesis that C1q influences microglial state. Indeed, we show that C1q increases fatty acid storage in iMGL as LPS does, consistent with an inflammatory phenotype. However, unlike LPS, we show that C1q also upregulates mitochondria membrane potential, suggesting C1q drives an iMGL phenotype that is distinct from that of LPS. This critically suggests that C1q treatment increases energy production in microglia and provides new function-based insight into how C1q is modulating microglial state. These data together identify C1q as a novel and unique molecular regulator of microglial state/function.

The complement cascade is a key part of the innate immune system's defense against pathogens, functioning by initiating a series of enzymatic reactions, recruiting inflammatory cells, tagging pathogens for removal, and triggering cell lysis. C1q, the recognition molecule of the classical complement cascade, has a well-defined role in recognizing antigens and pathogens, initiating autocatalytic activation of the complement cascade, and tagging debris for clearance by phagocytic immune cells. In addition to its traditional roles in the immune system, C1q as a single molecule has recently become recognized for novel functions within the CNS. Indeed, C1q induces ERK, mitogen-activated protein kinases, and Akt signaling pathways (Agostinis et al., 2010; Benavente et al., 2020; Lee et al., 2018), suggesting it could play a more complex role than opsonization of cells and debris. In support of this notion, C1q mediates neurodevelopmental plasticity by tagging low-activity presynaptic terminals for elimination by microglia (Schafer et al., 2012; Stevens et al., 2007), modulates axon growth by suppressing myelin-associated glycoprotein growth inhibitory signaling (Peterson et al., 2015), and serves as a chemotactic cue to initiate neural stem cell migration (Benavente et al., 2020).

C1q is present within the healthy and intact CNS, but is highly upregulated following aging (Stephan et al., 2013), injury (Figley et al., 2014), ischemia (Schäfer et al., 2000), Alzheimer's disease (Chatterjee et al., 2023), Parkinson's disease (Depboylu et al., 2011), and numerous other neurodegeneration conditions. These data suggest that C1q is likely to play a broad role in modulation of CNS inflammation in the context of disease and injury. In this regard, treatment of primary rat microglia cultures with exogenous C1q increases proinflammatory cytokine and nitric oxide release (Färber et al., 2009). Here, we show that C1q similarly increases human iMGL transcription of proinflammatory markers in a dose-dependent manner. Therefore, C1q in the diseased CNS is likely to modulate microglial inflammation associated with aging, neurodegenerative disease, and injury. Future studies will investigate this hypothesis by moving towards a chimeric mouse model in which iMGL are transplanted into xenotolerant mice. The advantage of these in vivo studies lies in the fact that human microglia receive complex, in vivo cues and can successfully recapitulate the morphological regional diversity observed in murine microglia (Grabert et al., 2016; Hasselmann et al., 2019). These next set of studies will likely provide important additional data regarding the potential regional specific effects on human microglia that are likely to occur in vivo.

Overall, the data in this manuscript establish a novel tool to investigate changes in microglial organelles and thus provide insight into changes in microglial function. While traditional transcriptomic and proteomic tools are powerful, they provide only a limited understanding of these complex immune cells. Future studies will combine traditional evaluations of gene and protein signature with this novel organelle phenotyping approach to better characterize microglial responses to disease and treatment. For example, this tool provides us with the capacity to probe how different patient derived microglia respond to disease stimulations (i.e., Aβ plaques, tau tangles, and alpha-synuclein) and how the same patient lines respond to potential pharmaceutical interventions. This combination will ultimately enable enhanced investigation of microglial state at the RNA, protein, and functional level. Taken together, this platform has the capacity to inform both basic science investigation and personalized medicine by providing a tool that will efficiently probe microglial state and function.

AUTHOR CONTRIBUTIONS

Pooja S. Sakthivel: Conceptualization; methodology; funding acquisition; writing – original draft; writing – review and editing; investigation; formal analysis; data curation. **Lorenzo Scipioni:** Conceptualization; methodology; data curation; investigation; formal analysis. **Josh Karam:** Methodology; investigation; data curation. **Zahara Keulen:** Methodology; investigation. **Mathew Blurton-Jones:** Supervision; methodology. **Enrico Gratton:** Supervision; methodology. **Aileen J. Anderson:** Funding acquisition; conceptualization; methodology; supervision; writing – original draft; writing – review and editing.

ACKNOWLEDGMENTS

The authors are grateful to Vanessa Scarfone and Pauline Nguyen at the UCI Stem Cell Center Flow Cytometry Core for their guidance and expertise. Research reported in this publication was supported by the National Institute of Neurological Disorders and Stroke of the National Institutes of Health under Award Numbers T32NS082174 and R01NS123927-01Q. The content is solely the responsibility of the authors and does not necessarily represent the official views of the National Institutes of Health. Graphical abstract was created with BioRender (https://biorender.com/).

CONFLICT OF INTEREST STATEMENT

M.B.J. is a co-inventor on a pending patent filed by the University of California Regents (application 63/169578) related to genetic modification of cells to confer resistance to CSF1R antagonists. M.B.J. is a co-inventor of patent WO/2018/160496, related to the differentiation of human pluripotent stem cells into microglia. M.B.J. is a co-founder of NovoGlia Inc.

PEER REVIEW

The peer review history for this article is available at https://www.webofscience.com/api/gateway/wos/peer-review/10.1111/jnc.16173.

DATA AVAILABILITY STATEMENT

The data that support the findings of this study are available from the corresponding authors upon reasonable request. A preprint of this manuscript was posted on BioRxiv on the 13/12/2023 https://urldefense.com/v3/__https://www.biorxiv.org/content/10.1101/2023.12.12.571151v2__;!!CzAuKJ42GuquVTTmVmPViYEvSg!L8FS7WOYHMRnsmFIf44thhgYAvIDz6Ado3mNLhOIjpwWCVikGz1vzs8Anq3FuRgDrqJTNJ33-ghBq2CzwdE2kwFD$.

ORCID

Pooja S. Sakthivel https://orcid.org/0000-0002-1422-4609

REFERENCES

Agostinis, C., Bulla, R., Tripodo, C., Gismondi, A., Stabile, H., Bossi, F., Guarnotta, C., Garlanda, C., De Seta, F., Spessotto, P., Santoni, A., Ghebrehiwet, B., Girardi, G., & Tedesco, F. (2010). An alternative role of C1q in cell migration and tissue remodeling: Contribution to trophoblast invasion and placental development. *Journal of Immunology (Baltimore, Md.:1950)*, *185*(7), 4420–4429. https://doi.org/10.4049/jimmunol.0903215

Au, N. P. B., & Ma, C. H. E. (2017). Recent advances in the study of bipolar/rod-shaped microglia and their roles in neurodegeneration. *Frontiers in Aging Neuroscience*, *9*, 128. https://doi.org/10.3389/fnagi.2017.00128

Benavente, F., Piltti, K. M., Hooshmand, M. J., Nava, A. A., Lakatos, A., Feld, B. G., Creasman, D., Gershon, P. D., & Anderson, A. (2020). Novel C1q receptor-mediated signaling controls neural stem cell behavior and neurorepair. *eLife*, *9*, e55732. https://doi.org/10.7554/eLife.55732

Block, M. L., Zecca, L., & Hong, J.-S. (2007). Microglia-mediated neurotoxicity: Uncovering the molecular mechanisms. *Nature Reviews Neuroscience*, *8*(1), 57–69. https://doi.org/10.1038/nrn2038

Burns, T. C., Li, M. D., Mehta, S., Awad, A. J., & Morgan, A. A. (2015). Mouse models rarely mimic the transcriptome of human neurodegenerative diseases: A systematic bioinformatics-based critique of preclinical models. *European Journal of Pharmacology*, *759*, 101–117. https://doi.org/10.1016/j.ejphar.2015.03.021

Button, E. B., Mitchell, A. S., Domingos, M. M., Chung, J. H.-J., Bradley, R. M., Hashemi, A., Marvyn, P. M., Patterson, A. C., Stark, K. D., Quadrilatero, J., & Duncan, R. E. (2014). Microglial cell activation increases saturated and decreases monounsaturated fatty acid content, but both lipid species are proinflammatory. *Lipids*, *49*(4), 305–316. https://doi.org/10.1007/s11745-014-3882-y

Chatterjee, M., Özdemir, S., Kunadt, M., Koel-Simmelink, M., Boiten, W., Piepkorn, L., Pham, T. V., Chiasserini, D., Piersma, S. R., Knol, J. C., Möbius, W., Mollenhauer, B., Van Der Flier, W. M., Jimenez, C. R., Teunissen, C. E., Jahn, O., & Schneider, A. (2023). C1q is increased in cerebrospinal fluid-derived extracellular vesicles in Alzheimer's disease: A multi-cohort proteomics and immuno-assay validation study. *Alzheimer's & Dementia*, *19*(11), 4828–4840. https://doi.org/10.1002/alz.13066

D'Avila, H., Maya-Monteiro, C. M., & Bozza, P. T. (2008). Lipid bodies in innate immune response to bacterial and parasite infections. *International Immunopharmacology*, *8*(10), 1308–1315. https://doi.org/10.1016/j.intimp.2008.01.035

Depboylu, C., Schäfer, M. K.-H., Arias-Carrión, O., Oertel, W. H., Weihe, E., & Höglinger, G. U. (2011). Possible involvement of complement factor C1q in the clearance of extracellular Neuromelanin from the substantia Nigra in Parkinson disease. *Journal of Neuropathology & Experimental Neurology*, *70*(2), 125–132. https://doi.org/10.1097/NEN.0b013e31820805b9

Dolan, M.-J., Therrien, M., Jereb, S., Kamath, T., Gazestani, V., Atkeson, T., Marsh, S. E., Goeva, A., Lojek, N. M., Murphy, S., White, C. M., Joung, J., Liu, B., Limone, F., Eggan, K., Hacohen, N., Bernstein, B. E., Glass, C. K., Leinonen, V., … Stevens, B. (2023). Exposure of iPSC-derived human microglia to brain substrates enables the generation and manipulation of diverse transcriptional states in vitro. *Nature Immunology*, *24*(8), 1382–1390. https://doi.org/10.1038/s41590-023-01558-2

Färber, K., Cheung, G., Mitchell, D., Wallis, R., Weihe, E., Schwaeble, W., & Kettenmann, H. (2009). C1q, the recognition subcomponent of the classical pathway of complement, drives microglial activation. *Journal of Neuroscience Research*, *87*(3), 644–652. https://doi.org/10.1002/jnr.21875

Figley, S. A., Khosravi, R., Legasto, J. M., Tseng, Y.-F., & Fehlings, M. G. (2014). Characterization of vascular disruption and blood-spinal cord barrier permeability following traumatic spinal cord injury. *Journal of Neurotrauma*, *31*(6), 541–552. https://doi.org/10.1089/neu.2013.3034

Fraser, D. A., Pisalyaput, K., & Tenner, A. J. (2010). C1q enhances microglial clearance of apoptotic neurons and neuronal blebs, and modulates subsequent inflammatory cytokine production. *Journal of Neurochemistry*, *112*(3), 733–743. https://doi.org/10.1111/j.1471-4159.2009.06494.x

Freria, C. M., Hall, J. C. E., Wei, P., Guan, Z., McTigue, D. M., & Popovich, P. G. (2017). Deletion of the Fractalkine receptor, CX3CR1, improves endogenous repair, axon sprouting, and synaptogenesis after spinal cord injury in mice. *The Journal of Neuroscience: The Official Journal of the Society for Neuroscience*, *37*(13), 3568–3587. https://doi.org/10.1523/JNEUROSCI.2841-16.2017

Grabert, K., Michoel, T., Karavolos, M. H., Clohisey, S., Baillie, J. K., Stevens, M. P., Freeman, T. C., Summers, K. M., & McColl, B. W. (2016). Microglial brain region-dependent diversity and selective regional sensitivities to aging. *Nature Neuroscience*, *19*(3), 504–516. https://doi.org/10.1038/nn.4222

Hakim, R., Zachariadis, V., Sankavaram, S. R., Han, J., Harris, R. A., Brundin, L., Enge, M., & Svensson, M. (2021). Spinal cord injury induces permanent re-programming of microglia into a disease-associated state which contributes to functional recovery. *The Journal of Neuroscience*, *41*, 8459. https://doi.org/10.1523/JNEUROSCI.0860-21.2021

Hasselmann, J., Coburn, M. A., England, W., Figueroa Velez, D. X., Kiani Shabestari, S., Tu, C. H., McQuade, A., Kolahdouzan, M., Echeverria, K., Claes, C., Nakayama, T., Azevedo, R., Coufal, N. G., Han, C. Z., Cummings, B. J., Davtyan, H., Glass, C. K., Healy, L. M., Gandhi, S. P., … Blurton-Jones, M. (2019). Development of a chimeric model to study and manipulate human microglia in vivo. *Neuron*, *103*(6), 1016–1033, e10. https://doi.org/10.1016/j.neuron.2019.07.002

Ho, C.-Y., Lin, Y.-T., Chen, H.-H., Ho, W.-Y., Sun, G.-C., Hsiao, M., Lu, P.-J., Cheng, P.-W., & Tseng, C.-J. (2020). CX3CR1-microglia mediates neuroinflammation and blood pressure regulation in the nucleus tractus solitarii of fructose-induced hypertensive rats. *Journal of Neuroinflammation*, *17*(1), 185. https://doi.org/10.1186/s12974-020-01857-7

Hooshmand, M. J., Nguyen, H. X., Piltti, K. M., Benavente, F., Hong, S., Flanagan, L., Uchida, N., Cummings, B. J., & Anderson, A. J. (2017). Neutrophils induce Astroglial differentiation and migration of human neural stem cells via C1q and C3a synthesis. *The Journal of Immunology*, *199*(3), 1069–1085. https://doi.org/10.4049/jimmunol.1600064

Keren-Shaul, H., Spinrad, A., Weiner, A., Matcovitch-Natan, O., Dvir-Szternfeld, R., Ulland, T. K., David, E., Baruch, K., Lara-Astaiso, D., Toth, B., Itzkovitz, S., Colonna, M., Schwartz, M., & Amit, I. (2017). A unique microglia type associated with restricting development of Alzheimer's disease. *Cell*, *169*(7), 1276–1290.e17. https://doi.org/10.1016/j.cell.2017.05.018

Khatchadourian, A., Bourque, S. D., Richard, V. R., Titorenko, V. I., & Maysinger, D. (2012). Dynamics and regulation of lipid droplet formation in lipopolysaccharide (LPS)-stimulated microglia. *Biochimica et Biophysica Acta*, *1821*(4), 607–617. https://doi.org/10.1016/j.bbalip.2012.01.007

Koussounadis, A., Langdon, S. P., Um, I. H., Harrison, D. J., & Smith, V. A. (2015). Relationship between differentially expressed mRNA and mRNA-protein correlations in a xenograft model system. *Scientific Reports*, *5*(1), 10775. https://doi.org/10.1038/srep10775

Kuna, P., Iyer, M., Peerschke, E. I., Kaplan, A. P., Reid, K. B., & Ghebrehiwet, B. (1996). Human C1q induces eosinophil migration. *Clinical Immunology and Immunopathology*, *81*(1), 48–54. https://doi.org/10.1006/clin.1996.0156

Lee, J.-H., Poudel, B., Ki, H.-H., Nepali, S., Lee, Y.-M., Shin, J.-S., & Kim, D.-K. (2018). Complement C1q stimulates the progression of hepatocellular tumor through the activation of discoidin domain receptor 1. *Scientific Reports*, *8*(1), 4908. https://doi.org/10.1038/s41598-018-23240-6

Majumdar, A., Cruz, D., Asamoah, N., Buxbaum, A., Sohar, I., Lobel, P., & Maxfield, F. R. (2007). Activation of microglia acidifies lysosomes and leads to degradation of Alzheimer amyloid fibrils. *Molecular Biology of the Cell*, *18*(4), 1490–1496. https://doi.org/10.1091/mbc.e06-10-0975

McQuade, A., Coburn, M., Tu, C. H., Hasselmann, J., Davtyan, H., & Blurton-Jones, M. (2018). Development and validation of a simplified method to generate human microglia from pluripotent stem cells. *Molecular Neurodegeneration*, *13*(1), 67. https://doi.org/10.1186/s13024-018-0297-x

Michelucci, A., Heurtaux, T., Grandbarbe, L., Morga, E., & Heuschling, P. (2009). Characterization of the microglial phenotype under specific pro-inflammatory and anti-inflammatory conditions: Effects of oligomeric and fibrillar amyloid-β. *Journal of Neuroimmunology*, *210*(1–2), 3–12. https://doi.org/10.1016/j.jneuroim.2009.02.003

Nimmerjahn, A., Kirchhoff, F., & Helmchen, F. (2005). Resting microglial cells are highly dynamic surveillants of brain parenchyma in vivo. *Science*, *308*, 6.

Paolicelli, R. C., Sierra, A., Stevens, B., Tremblay, M.-E., Aguzzi, A., Ajami, B., Amit, I., Audinat, E., Bechmann, I., Bennett, M., Bennett, F., Bessis, A., Biber, K., Bilbo, S., Blurton-Jones, M., Boddeke, E., Brites, D., Brône, B., Brown, G. C., … Wyss-Coray, T. (2022). Microglia states and nomenclature: A field at its crossroads. *Neuron*, *110*(21), 3458–3483. https://doi.org/10.1016/j.neuron.2022.10.020

Peterson, S. L., Nguyen, H. X., Mendez, O. A., & Anderson, A. J. (2015). Complement protein C1q modulates neurite outgrowth in vitro and spinal cord axon regeneration in vivo. *Journal of Neuroscience*, *35*(10), 4332–4349. https://doi.org/10.1523/JNEUROSCI.4473-12.2015

Polazzi, E., & Contestabile, A. (2002). Reciprocal interactions between microglia and neurons: From survival to neuropathology. *Reviews in the Neurosciences*, *13*(3), 221–242. https://doi.org/10.1515/REVNEURO.2002.13.3.221

Quick, J. D., Silva, C., Wong, J. H., Lim, K. L., Reynolds, R., Barron, A. M., Zeng, J., & Lo, C. H. (2023). Lysosomal acidification dysfunction in microglia: An emerging pathogenic mechanism of neuroinflammation and neurodegeneration. *Journal of Neuroinflammation*, *20*(1), 185. https://doi.org/10.1186/s12974-023-02866-y

Rajbhandari, P., Thomas, B. J., Feng, A.-C., Hong, C., Wang, J., Vergnes, L., Sallam, T., Wang, B., Sandhu, J., Seldin, M. M., Lusis, A. J., Fong, L. G., Katz, M., Lee, R., Young, S. G., Reue, K., Smale, S. T., & Tontonoz, P. (2018). IL-10 signaling remodels adipose chromatin architecture to limit thermogenesis and energy expenditure. *Cell*, *172*(1–2), 218–233, e17. https://doi.org/10.1016/j.cell.2017.11.019

Ransohoff, R. M. (2016). A polarizing question: Do M1 and M2 microglia exist? *Nature Neuroscience*, *19*(8), 987–991. https://doi.org/10.1038/nn.4338

Safaiyan, S., Besson-Girard, S., Kaya, T., Cantuti-Castelvetri, L., Liu, L., Ji, H., Schifferer, M., Gouna, G., Usifo, F., Kannaiyan, N., Fitzner, D., Xiang, X., Rossner, M. J., Brendel, M., Gokce, O., & Simons, M. (2021). White matter aging drives microglial diversity. *Neuron*, *109*(7), 1100–1117, e10. https://doi.org/10.1016/j.neuron.2021.01.027

Sala Frigerio, C., Wolfs, L., Fattorelli, N., Thrupp, N., Voytyuk, I., Schmidt, I., Mancuso, R., Chen, W.-T., Woodbury, M. E., Srivastava, G., Möller, T., Hudry, E., Das, S., Saido, T., Karran, E., Hyman, B., Perry, V. H., Fiers, M., & De Strooper, B. (2019). The major risk factors for Alzheimer's disease: Age, sex, and genes modulate the microglia response to Aβ plaques. *Cell Reports*, *27*(4), 1293–1306, e6. https://doi.org/10.1016/j.celrep.2019.03.099

Schafer, D. P., Lehrman, E. K., Kautzman, A. G., Koyama, R., Mardinly, A. R., Yamasaki, R., Ransohoff, R. M., Greenberg, M. E., Barres, B. A., & Stevens, B. (2012). Microglia sculpt postnatal neural circuits in an activity and complement-dependent manner. *Neuron*, *74*(4), 691–705. https://doi.org/10.1016/j.neuron.2012.03.026

Schäfer, M. K.-H., Schwaeble, W. J., Post, C., Salvati, P., Calabresi, M., Sim, R. B., Petry, F., Loos, M., & Weihe, E. (2000). Complement C1q is dramatically up-regulated in brain microglia in response to transient global cerebral ischemia. *The Journal of Immunology*, *164*(10), 5446–5452. https://doi.org/10.4049/jimmunol.164.10.5446

Scipioni, L., Tedeschi, G., Navarro, M., Jia, Y., Atwood, S., Prescher, J. A., & Digman, M. (2024). *ESPRESSO: Spatiotemporal omics based on organelle phenotyping*. https://doi.org/10.1101/2024.06.13.598932

Seok, J., Warren, H. S., Cuenca, A. G., Mindrinos, M. N., Baker, H. V., Xu, W., Richards, D. R., McDonald-Smith, G. P., Gao, H., Hennessy, L., Finnerty, C. C., López, C. M., Honari, S., Moore, E. E., Minei, J. P., Cuschieri, J., Bankey, P. E., Johnson, J. L., Sperry, J., … Wong, W. H. (2013). Genomic responses in mouse models poorly mimic human inflammatory diseases. *Proceedings of the National Academy of Sciences*, *110*(9), 3507–3512. https://doi.org/10.1073/pnas.1222878110

Shen, J., Liu, Y., Ren, X., Gao, K., Li, Y., Li, S., Yao, J., & Yang, X. (2016). Changes in DNA methylation and chromatin structure of pro-inflammatory cytokines stimulated by LPS in broiler peripheral blood mononuclear cells. *Poultry Science*, *95*(7), 1636–1645. https://doi.org/10.3382/ps/pew086

Singh, R., Kaushik, S., Wang, Y., Xiang, Y., Novak, I., Komatsu, M., Tanaka, K., Cuervo, A. M., & Czaja, M. J. (2009). Autophagy regulates lipid metabolism. *Nature*, *458*(7242), 1131–1135. https://doi.org/10.1038/nature07976

Stephan, A. H., Madison, D. V., Mateos, J. M., Fraser, D. A., Lovelett, E. A., Coutellier, L., Kim, L., Tsai, H.-H., Huang, E. J., Rowitch, D. H., Berns, D. S., Tenner, A. J., Shamloo, M., & Barres, B. A. (2013). A dramatic increase of C1q protein in the CNS during normal aging. *Journal of Neuroscience*, *33*(33), 13460–13474. https://doi.org/10.1523/JNEUROSCI.1333-13.2013

Stevens, B., Allen, N. J., Vazquez, L. E., Howell, G. R., Christopherson, K. S., Nouri, N., Micheva, K. D., Mehalow, A. K., Huberman, A. D., Stafford, B., Sher, A., Litke, A. M., Lambris, J. D., Smith, S. J., John, S. W. M., & Barres, B. A. (2007). The classical complement cascade mediates CNS synapse elimination. *Cell*, *131*(6), 1164–1178. https://doi.org/10.1016/j.cell.2007.10.036

Tremblay, M.-È., Lecours, C., Samson, L., Sánchez-Zafra, V., & Sierra, A. (2015). From the Cajal alumni Achúcarro and Río-Hortega to the rediscovery of never-resting microglia. *Frontiers in Neuroanatomy*, *9*, 2. https://doi.org/10.3389/fnana.2015.00045

Vogel, D. Y. S., Heijnen, P. D. A. M., Breur, M., de Vries, H. E., Tool, A. T. J., Amor, S., & Dijkstra, C. D. (2014). Macrophages migrate in an activation-dependent manner to chemokines involved in neuroinflammation. *Journal of Neuroinflammation*, *11*, 23. https://doi.org/10.1186/1742-2094-11-23

Voloboueva, L. A., Emery, J. F., Sun, X., & Giffard, R. G. (2013). Inflammatory response of microglial BV-2 cells includes a glycolytic shift and is modulated by mitochondrial glucose-regulated protein

75/mortalin. *FEBS Letters*, *587*(6), 756–762. https://doi.org/10.1016/j.febslet.2013.01.067

Yasojima, K., Schwab, C., McGeer, E. G., & McGeer, P. L. (1999). Up-regulated production and activation of the complement system in Alzheimer's disease brain. *The American Journal of Pathology*, *154*(3), 927–936. https://doi.org/10.1016/S0002-9440(10)65340-0

Yi, S., Jiang, X., Tang, X., Li, Y., Xiao, C., Zhang, J., & Zhou, T. (2020). IL-4 and IL-10 promotes phagocytic activity of microglia by up-regulation of TREM2. *Cytotechnology*, *72*(4), 589–602. https://doi.org/10.1007/s10616-020-00409-4

Zabel, M. K., Zhao, L., Zhang, Y., Gonzalez, S. R., Ma, W., Wang, X., Fariss, R. N., & Wong, W. T. (2016). Microglial phagocytosis and activation underlying photoreceptor degeneration is regulated by CX3CL1-CX3CR1 signaling in a mouse model of retinitis pigmentosa. *Glia*, *64*(9), 1479–1491. https://doi.org/10.1002/glia.23016

Zhang, H. (2011). Microglia-friend or foe. *Frontiers in Bioscience*, *S3*(1), 869. https://doi.org/10.2741/193

How to cite this article: Sakthivel, P. S., Scipioni, L., Karam, J., Keulen, Z., Blurton-Jones, M., Gratton, E., & Anderson, A. J. (2024). Organelle phenotyping and multi-dimensional microscopy identify C1q as a novel regulator of microglial function. *Journal of Neurochemistry*, *00*, 1–13. https://doi.org/10.1111/jnc.16173